

ANALYSIS OF A NATURAL FREQUENCY TRACKING SYSTEM FOR MEMS FATIGUE TESTING

Xiaotian Sun, Roberto Horowitz, and Kyriakos Komvopoulos*

Department of Mechanical Engineering

University of California

Berkeley, CA 94720

Email: kyriakos@me.berkeley.edu

ABSTRACT

A nonlinear control system that can track the natural frequency of a MEMS resonator was developed in this study. Due to the evolution of fatigue damage, the natural frequency of the resonator decreases. To maintain the device at resonance, a phase-locked loop system is used to track the frequency decay and adjust the driving force accordingly. A model for the control system is introduced and the system behavior is analyzed using an averaging method. A quantitative criterion for selecting the control gain to achieve stability is derived from the analysis. Simulation results are shown to be in good agreement with the prediction of the theoretical analysis.

1 INTRODUCTION

Tracking the natural frequency of microelectromechanical system (MEMS) devices is a critical task that may be complicated by a variety of factors, such as degradation of the material integrity. Of particular significance is the tracking ability of the natural frequency decay of an oscillating MEMS device due to fatigue damage. As in macroscopic mechanical devices, fatigue is also an important factor in miniature devices like MEMS resonators. Understanding of the fatigue mechanism of MEMS structural materials is of great importance in reliability analysis of microsystems and influences micromachine operation and robustness. Since fatigue damage at the microscale has attracted the attention of researchers only recently, there is a great demand for control schemes enabling fast tracking of the dynamic behav-

ior of resonating microdevices.

To investigate fatigue under cyclic loading in MEMS devices, a two-layer polycrystalline silicon resonator [1], such as that shown in Figure 1, was fabricated using the MUMPS process [2]. The beams at the center of the device, attached to an anchor and a rotating ring, are the testing samples. These flexure beams are bended when the shutters of the comb drives rotate functioning as the spring of the resonator. The comb drives are divided into two groups (marked by *A* and *B* in Figure 1), and the comb drives in each group are electrically connected via the two rings around the device. Group *A* of the comb drives is used to generate electrostatic forces that excite the resonator, while group *B* is used to sense the position of the shutter by measuring the capacitance change due to rotation.

Tracking the natural frequency during fatigue testing is crucial for the following reasons:

1. Large strains in the test samples can only be achieved at resonance. The MEMS resonators are lightly damped and have high quality factors (Q is equal to ~ 100 in air and can easily reach values in the range of 10^4 – 10^5 in vacuum). Thus, the large displacements needed to produce sufficient deformation can only be achieved at resonance, *i.e.*, at a frequency very close to the natural frequency of a lightly damped system.
2. The natural frequency decay is used to determine the decrease of the stiffness of the test samples due to fatigue damage. During cyclic loading, grains in the test samples may be damaged, causing the effective stiffness to decrease, and, in turn, a downward shift of the natural frequency. Hence,

*Address all correspondence to this author.

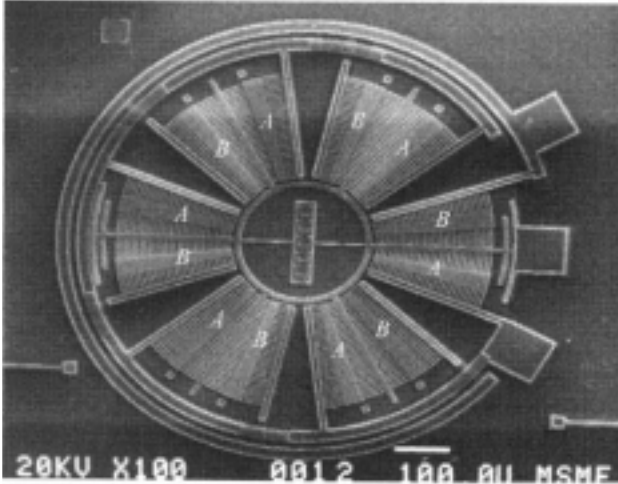


Figure 1. SEM image of a polycrystalline silicon MEMS resonator for fatigue test.

the characteristics of the fatigue process can be studied by observing the decay history of the natural frequency.

In this paper, a phase-locked loop (PLL) control scheme, which can closely track the natural frequency of the vibrating resonator, is analyzed and its tracking efficiency in the absence of noise is evaluated in light of simulation results. A fifth-order nonlinear dynamic model of the entire system including the PLL, the resonator, and the driving and sensing circuits is presented first. A simplified (although still nonlinear) system of dynamic equations is used to examine this nonlinear dynamic system. Excitation at the natural frequency yields a stable closed orbit of the original system only when a certain criterion for the control gain is satisfied. The validity of the analysis is interpreted in light of simulation results for the original system.

2 PHASE-LOCKED LOOP AND SYSTEM MODEL

A PLL consists of three functional blocks: a phase detector, a controller, and a voltage-controlled oscillator (VCO), as illustrated in Figure 2. The phase detector compares the phase difference between the reference and the output, and then feeds an error signal, which is proportional to the phase difference, to the controller. From this error signal, the controller calculates the control voltage of the VCO, and the oscillating frequency of the VCO is an affine function of this control voltage in the operating range. Thus, with a proper design of the controller, the output of the PLL will track the reference signal in both frequency and phase. Details regarding the operating principles of PLL can be found in [3].

For an analog PLL, a four-quadrant multiplier and a low-pass filter are often used as the phase detector, as in the system of this study. The block diagram of the entire system is shown

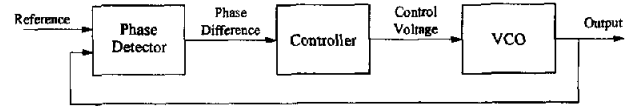


Figure 2. The block diagram of a phase-locked loop.

in Figure 3. The output of the PLL is first amplified and then fed to the driving combs of the resonator. The position of the resonator is measured by capacitive sensing circuits. The phase difference between the measured position signal and the excitation signal, which is the output of the VCO, is compared by the phase detector. The control voltage of the VCO is calculated by the controller from this phase difference. The equations describing the behaviors of these functional blocks are established next.

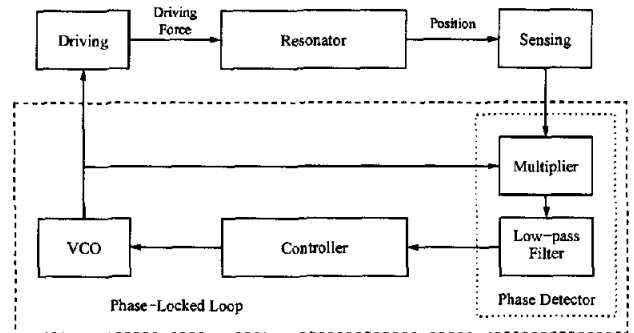


Figure 3. The block diagram of the natural frequency tracking system for a MEMS resonator.

The resonator is modeled as a second-order spring-mass-damper system, and its dynamic behavior is described by

$$\ddot{x} + c\dot{x} + \omega_n^2 x = F, \quad (1)$$

where x is the position, c is the normalized damping factor, ω_n is the natural frequency, and F is the normalized driving force. The driving force is an electrostatic force generated by the comb drives and is proportional (under proper bias) to the AC driving voltage, which is the amplified VCO output. The driving force can be written as

$$F = A \cos \theta, \quad (2)$$

where $\cos \theta$ is the output of the VCO, θ is the instantaneous phase, and A is the amplitude of the force, which is the product of the gain of the driving amplifier and the hardware gain (from voltage to force) of the comb drives.

By the architecture, the instantaneous frequency of the VCO is an affine function of the control voltage, z , of the VCO, which can be defined as:

$$\omega := \dot{\theta} = \omega_0 + K_{VCO}z, \quad (3)$$

where ω_0 is the free oscillation frequency. The instantaneous phase of the VCO is thus the integral of the instant frequency

$$\theta = \int_0^t (\omega_0 + K_{VCO}z) d\tau. \quad (4)$$

Let the control voltage of the VCO, z , be calculated from the output of the phase detector, y , by a proportional-integral controller,

$$z = K_P y + K_I \int_0^t y d\tau,$$

i.e.,

$$\dot{z} = K_P \dot{y} + K_I y, \quad (5)$$

where K_P and K_I are the proportional and integral control gains, respectively. The output of the phase detector is the product of the measured position signal, $K_G x$, and the VCO output, $\cos\theta$, filtered by a low-pass filter, *i.e.*,

$$\dot{y} = \lambda(K_G x \cos\theta - y), \quad (6)$$

where K_G is the gauge factor (from position to voltage) of the sensing combs and circuits, and λ is the corner frequency of the low-pass filter. Substituting (6) into (5) yields

$$\dot{z} = K_P K_G \lambda x \cos\theta + (K_I - K_P \lambda) y.$$

By letting $K_P = 0$, the above equation is simplified as

$$\dot{z} = K_I y. \quad (7)$$

In summary, the entire closed PLL natural frequency tracking system, shown in Figure 3, is described by (8)–(11):

$$\ddot{x} + c\dot{x} + \omega_n^2 x = A \cos\theta, \quad (8)$$

$$\dot{\theta} = \omega_0 + K_{VCO}z, \quad (9)$$

$$\dot{z} = K_I y, \quad (10)$$

$$\dot{y} = \lambda(K_G x \cos\theta - y). \quad (11)$$

3 ANALYSIS USING THE METHOD OF AVERAGING

In order to analyze the transient behavior of the system, the position of the resonator is defined as

$$x := a(t) \cos[\theta(t) + \phi(t)], \quad (12)$$

where $a(t)$ is the amplitude, and $\theta(t) + \phi(t)$ is the instantaneous phase of the resonator position signal, respectively. Separating the instantaneous phase of the VCO, θ , from the instantaneous phase of the shutter position, the phase difference between the VCO output and the resonator position is equal to ϕ . Differentiating (12) with respect to time gives the velocity

$$\dot{x} = -a\dot{\theta} \sin(\theta + \phi) + \dot{a} \cos(\theta + \phi) - a\dot{\phi} \sin(\theta + \phi). \quad (13)$$

Setting the sum of the last two terms to zero yields

$$\dot{a} \cos(\theta + \phi) - a\dot{\phi} \sin(\theta + \phi) \equiv 0, \quad (14)$$

which is one of the equations used to determine a and ϕ . Thus, the velocity equation becomes

$$\dot{x} = -a\dot{\theta} \sin(\theta + \phi). \quad (15)$$

The acceleration is obtained by differentiating (15) with respect to time,

$$\ddot{x} = -(\dot{a}\dot{\theta} + a\ddot{\theta}) \sin(\theta + \phi) - a\dot{\theta}(\dot{\theta} + \dot{\phi}) \cos(\theta + \phi). \quad (16)$$

Substituting (12), (15), and (16) into (8) yields

$$\begin{aligned} &-(\dot{a}\dot{\theta} + a\ddot{\theta}) \sin(\theta + \phi) \\ &- a(\dot{\theta}^2 - \omega_n^2 + \dot{\theta}\dot{\phi}) \cos(\theta + \phi) = A \cos\theta. \end{aligned} \quad (17)$$

Left-multiplying $\begin{bmatrix} \dot{\theta} \cos(\theta + \phi) - \sin(\theta + \phi) \\ \dot{\theta} \sin(\theta + \phi) \cos(\theta + \phi) \end{bmatrix}$, which is nonsingular when a trivial condition, $\dot{\theta} \neq 0$, is satisfied, to $\begin{bmatrix} (14) \\ (17) \end{bmatrix}$ yields

$$\begin{aligned} &a(\dot{\theta}^2 - \omega_n^2) \sin(\theta + \phi) \cos(\theta + \phi) + \dot{a}\dot{\theta} \\ &+ (a\ddot{\theta} + ca\dot{\theta}) \sin^2(\theta + \phi) = -A \sin(\theta + \phi) \cos\theta, \end{aligned} \quad (18)$$

$$\begin{aligned} &-(a\dot{\theta} + ca\dot{\theta}) \sin(\theta + \phi) \cos(\theta + \phi) - a\dot{\theta}\dot{\phi} \\ &- a(\dot{\theta}^2 - \omega_n^2) \cos^2(\theta + \phi) = A \cos(\theta + \phi) \cos\theta. \end{aligned} \quad (19)$$

From (9) and (10), we obtain

$$\ddot{\theta} = K_{VCO}\dot{z} = K_{VCO}K_I y. \quad (20)$$

By substituting (20) and (9) into (18) and (19), reordering terms, and including (10) and (11) yields

$$\begin{aligned} \dot{a} = & -\frac{1}{\omega_0 + K_{VCO}z} \left\{ A \sin(\theta + \phi) \cos \theta \right. \\ & + a \left[K_{VCO}K_I y + c(\omega_0 + K_{VCO}z) \right] \sin^2(\theta + \phi) \\ & \left. + a \left[(\omega_0 + K_{VCO}z)^2 - \omega_n^2 \right] \sin(\theta + \phi) \cos(\theta + \phi) \right\}, \end{aligned} \quad (21)$$

$$\begin{aligned} \dot{\phi} = & -\frac{1}{\omega_0 + K_{VCO}z} \left\{ \frac{A}{a} \cos(\theta + \phi) \cos \theta \right. \\ & + \left[K_{VCO}K_I y + c(\omega_0 + K_{VCO}z) \right] \sin(\theta + \phi) \cos(\theta + \phi) \\ & \left. + \left[(\omega_0 + K_{VCO}z)^2 - \omega_n^2 \right] \cos^2(\theta + \phi) \right\}, \end{aligned} \quad (22)$$

$$\dot{z} = K_I y, \quad (23)$$

$$\dot{y} = \lambda \left[K_G a \cos(\theta + \phi) \cos \theta - y \right]. \quad (24)$$

It should be noted that (21)–(24) are the exact differential equations describing the evolution of the amplitude and phase of the resonator position, as well as that of the internal states of the low-pass filter and controller. However, these equations are difficult to analyze because they are substantially non-autonomous. The instantaneous phase of the VCO, θ , can be regarded as a “normalized time”. Thus, the vector field of (21)–(24) can be regarded as an explicit function of time. However, since θ changes much faster than the other variables, such as a , ϕ , z , and y , functions $\sin(\theta + \phi)$ and $\cos(\theta + \phi)$ are almost periodic, and within a period, variables other than θ change very little. Hence, it is possible to apply the averaging method [4, 5] to the non-autonomous system (21)–(24) and approximate it by an autonomous system. M’Closkey and Vakakis [6] successfully analyzed a microresonator automatic gain control loop by using the method of averaging.

The averaged autonomous equations are

$$\begin{aligned} \dot{\bar{a}} = & -\frac{1}{\omega_0 + K_{VCO}\bar{z}} \left\{ \frac{A}{2} \sin \bar{\phi} \right. \\ & \left. + \frac{\bar{a}}{2} \left[K_{VCO}K_I \bar{y} + c(\omega_0 + K_{VCO}\bar{z}) \right] \right\}, \end{aligned} \quad (25)$$

$$\begin{aligned} \dot{\bar{\phi}} = & -\frac{1}{\omega_0 + K_{VCO}\bar{z}} \left\{ \frac{A}{2\bar{a}} \cos \bar{\phi} \right. \\ & \left. + \frac{1}{2} \left[(\omega_0 + K_{VCO}\bar{z})^2 - \omega_n^2 \right] \right\}, \end{aligned} \quad (26)$$

$$\dot{\bar{z}} = K_I \bar{y}, \quad (27)$$

$$\dot{\bar{y}} = \lambda \left(\frac{K_G}{2} \bar{a} \cos \bar{\phi} - \bar{y} \right), \quad (28)$$

where the bars denote averaged variables. These differential equations describe approximately how the displacement amplitude and phase evolve with time. Although still nonlinear, (25)–(28) are easier to analyze.

Since the amplitude $a \geq 0$, the equilibrium of the averaged system (25)–(28) is described by

$$\begin{aligned} \bar{a}_0 = \frac{A}{c\omega_n}, & & \bar{\phi}_0 = -\frac{\pi}{2}, \\ \bar{z}_0 = \frac{\omega_n - \omega_0}{K_{VCO}}, & & \bar{y}_0 = 0, \end{aligned}$$

while the oscillating frequency of the resonator, as well as that of the VCO, at this equilibrium, $\dot{\theta} = \omega_n$, is the natural frequency of the resonator.

The Jacobian matrix of the nonlinear dynamic system (25)–(28) at equilibrium is

$$\nabla f(\bar{a}_0, \bar{\phi}_0, \bar{z}_0, \bar{y}_0) = \begin{bmatrix} -\frac{c}{2} & 0 & -\frac{AK_{VCO}}{2\omega_n^2} & -\frac{AK_{VCO}K_I}{2c\omega_n^2} \\ 0 & -\frac{c}{2} & -K_{VCO} & 0 \\ 0 & 0 & 0 & K_I \\ 0 & \frac{AK_G}{2c\omega_n} & 0 & -\lambda \end{bmatrix}, \quad (29)$$

and its characteristic equation is

$$\left(\gamma + \frac{c}{2} \right) \left[\gamma^3 + \left(\lambda + \frac{c}{2} \right) \gamma^2 + \frac{\lambda c}{2} \gamma + \frac{AK_G K_{VCO} K_I}{2c\omega_n} \right] = 0, \quad (30)$$

where γ is the variable of the characteristic equation. All the eigenvalues of the linearized averaged system are asymptotically stable, if and only if the product of the inner two coefficients is larger than that of the outer two coefficients, *i.e.*,

$$c \left(\lambda + \frac{c}{2} \right) > \frac{AK_G K_{VCO} K_I}{c\omega_n}. \quad (31)$$

Based on the indirect method of Lyapunov, it is concluded that the equilibrium of the nonlinear averaged system is asymptotically stable within a neighborhood if and only if (31) is satisfied. For the original exact differential equations, this means that the solution of oscillation at the resonator’s natural frequency is stable and attractive, *i.e.*, for some initial excitation at a frequency within a certain range around the resonator’s natural frequency, the PLL control system will adjust the excitation frequency to the natural frequency. (31) provides a criterion for selecting the integral control gain, K_I , according to other parameters of the system, such as the hardware gains, K_{VCO} , K_G and A , and the damping factor, c .

4 SIMULATION RESULTS

The validity of criterion (31) was verified by simulating the original exact nonlinear differential equations (8)–(11) for different values of K_I . The numerical values of the parameters used in the simulation are listed in Table 1. From these values, the critical value of the integral control gain, K_{I0} is found to be equal to 23.4. Figure 4 shows how the excitation frequency tracks the natural frequency with $K_I = 20 < K_{I0}$, while Figure 5 shows the unstable behavior of the excitation frequency when $K_I = 25 > K_{I0}$. These simulation results demonstrate the validity of the derived criterion for selecting the integral control gain.

Table 1. Numerical values of the parameters used in the simulation.

Parameter	Value
A	100 N/kg
K_G	1×10^6 V/m
K_{VCO}	1×10^4 Hz/V
λ	628 rad/s
c	628 s^{-1}
ω_n	6.28×10^4 rad/s

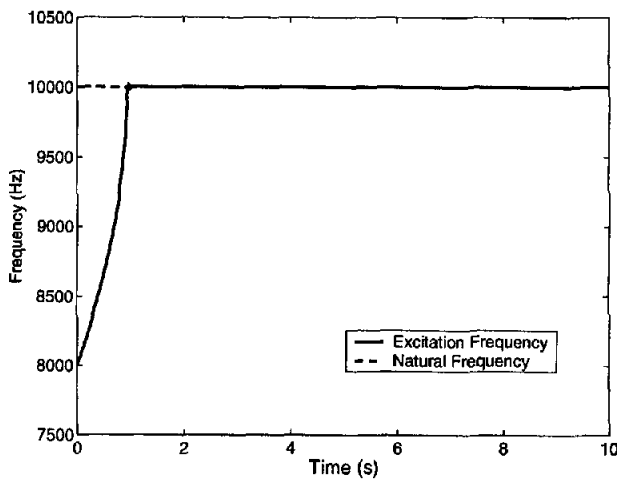


Figure 4. The excitation frequency tracks the natural frequency when $K_I = 20 < 23.4 = K_{I0}$.

Tracking the decaying natural frequency due to fatigue of the MEMS polycrystalline silicon spring was also simulated. It was assumed that the natural frequency decreases exponentially, *i.e.*,

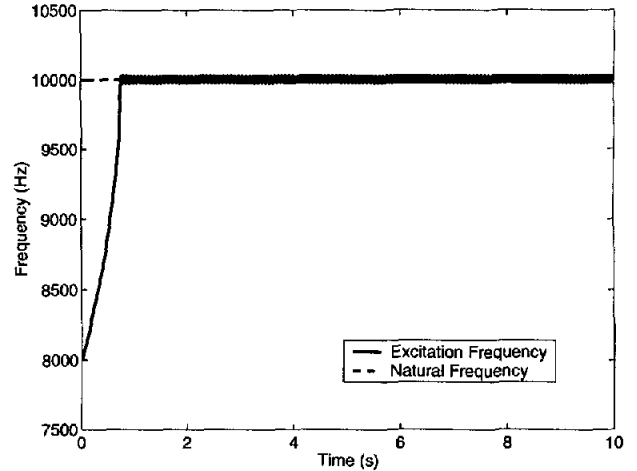


Figure 5. The excitation frequency oscillates about the natural frequency when $K_I = 25 > 23.4 = K_{I0}$.

$\omega_n = \omega_{n0}e^{-\alpha t}$, with a decay rate $\alpha = 0.01$. A rapid decrease of the natural frequency due to a sudden gain failure is also possible. Figure 6 shows how the excitation frequency tracks the decaying natural frequency for $K_I = 10$. This decay rate might be much faster than what is expected in fatigue experiments. Preliminary test results have shown that the resonant frequency of the two-beam microstructure shown in Figure 1 ($50 \mu\text{m}$ beam length with $4 \times 2 \mu\text{m}$ cross-section) decreases by 0.2 kHz after oscillating at resonance with displacement amplitude of $\sim 3 \mu\text{m}$ for 60 h. It can be seen from Figure 6 that the tracking performance, even for this fast decay, is satisfactory. This simulation result demonstrates the capability of the control system to efficiently track changes in the natural frequency of fatiguing microdevices. It should be pointed out that the tracking accuracy of the PLL control scheme could be affected by noise in the system, such as thermal noise in the capacitive sensing circuits and Brownian noise. The effects of such noise sources on the control system's steady-state resolution for the present microdevice has been shown to be negligibly small [7].

5 CONCLUSIONS

A phase-locked loop control system for tracking the natural frequency of a MEMS resonator was presented, and the dynamic equations describing this system were analyzed using a method of averaging. Based on the analysis, a criterion for selecting the control gain was established and its validity and effectiveness were verified by simulation results with the control gain satisfying or violating the stability criterion.

An extension to the work presented in this paper is to analyze the effect of noise on the tracking resolution. The sources of noise include the fundamental Brownian noise in the mechanical

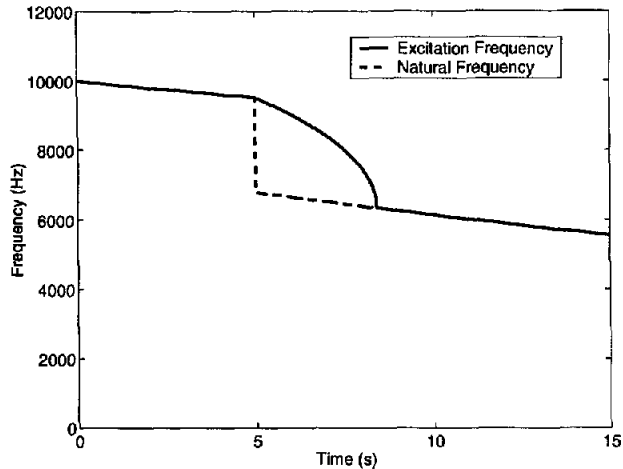


Figure 6. The excitation frequency tracks the decay of the resonator natural frequency, with $K_I = 10$.

structure and the thermal noise in the capacitive position sensing circuits. This analysis is currently carried out by the authors.

ACKNOWLEDGEMENT

This work was supported by the Defense Advanced Research Projects Agency (DARPA) under Grant No. DABT63-98-1-0011 and the National Science Foundation under Grant

No. DMI-9872324.

REFERENCES

1. Komvopoulos, K., 2001, "Microelectromechanical Structures for Multiaxial Fatigue Testing," *Proceedings of 10th International Congress of Fracture*.
2. Markus, K. W., Koester, D. A., Cowen, A., Mahadevan, R., Dhuler, V. R., Roberson, D., and Smith, L., 1995, "MEMS Infrastructure: The Multi-User MEMS Processes (MUMPs)," *Proceedings of SPIE: Micromachining and Microfabrication Process Technology*, vol. 2639, The International Society for Optical Engineering, Austin, TX, USA.
3. Best, R. E., 1999, *Phase-Locked Loops: Theory, Design, and Applications*, 4th ed., McGraw-Hill, New York.
4. Sanders, J. A., and Verhulst, F., 1985, *Averaging Methods in Nonlinear Dynamical Systems*, Springer-Verlag, New York.
5. Hale, J. K., 1980, *Ordinary Differential Equations*, 2nd ed., Krieger, Huntington, New York, USA.
6. M'Closkey, R. T., and Vakakis, A., 1999, "Analysis of a Microsensor Automatic Gain Control Loop," *Proceedings of the American Control Conference*, San Diego, California, USA.
7. Sun, X., Horowitz, R., and Komvopoulos, K., 2001, "Stability and Resolution Analysis of a Phase-Locked Loop Natural Frequency Tracking System for MEMS Fatigue Testing," *Journal of Microelectromechanical Systems*, submitted.